Significant portion of dissolved organic Fe complexes in fact is Fe colloids

Marie Boye [a,*,1], Jun Nishioka [b], Peter Croot [a,2], Patrick Laan [a], Klaas R. Timmermans [a], Volker H. Strass [c], Shigenobu Takeda [d], Hein J.W. de Baar [a]

[a] Royal Netherlands Institute for Sea Research (NIOZ), Postbus 59, 1790 AB Den Burg, Texel, The Netherlands
[b] Hokkaido University, Institute of Low Temperature Science, Sapporo 060-0819, Japan
[c] Alfred-Wegener-Institut für Polar und Meeresforschung, Bremerhaven, Germany
[d] University of Tokyo, Department of Aquatic Bioscience, Bunkyo, Tokyo 113-8657, Japan

ARTICLE INFO

ABSTRACT

Vertical distributions of iron and iron binding ligands were determined in 2 size classes (dissolved <0.2 μm, soluble <200 kDa, e.g., ~0.03 μm) in the Southern Ocean. Colloidal iron and complexing capacity (>200 kDa–<0.2 μm) were inferred as the difference between the dissolved and soluble fractions. Dissolved iron and ligands exist primarily in the soluble size range in the surface waters, although iron-complexing colloids still represent a significant portion of the dissolved pool and this fraction increases markedly with depth. This work presents evidence for the colloidal nature of a significant portion (37–51% on average) of the 'dissolved' organic Fe pool in these oceanic waters. From the data it was not possible to discern whether iron colloids exist as discrete organic complexes and/or inorganic amorphous colloids. Iron-complexing colloids are the most saturated with iron at the thermodynamic equilibrium, whereas soluble organic ligands occur in larger excess compared to soluble iron. It suggests that the exchangeable fraction for iron uptake through dissociation of Fe complexes likely occurs in the soluble fraction, and that soluble ligands have the potential to buffer iron inputs to surface waters whereas iron colloids may aggregate and settle. Expectations based on Fe diffusion rates, distributions and the stability of the soluble iron complexes and iron colloids also suggest that the weaker soluble Fe complexes may be more bio-available, while the strongest colloids may be a major route for iron removal from oceanic waters. Investigations of the size classes of the dissolved organic iron thus can significantly increase our understanding of the oceanic iron cycle.

1. Introduction

There is now compelling evidence to demonstrate that dissolved iron is principally complexed by organic ligands in oceanic waters (Gledhill and van den Berg, 1994; van den Berg, 1995; Rue and Bruland, 1995; Boye et al., 2001). The organic complexation is a central factor in oceanic iron cycling by controlling iron solubility (Wu and Luther, 1995) and selective iron bio-availability (Hutchins et al., 1999), but the speciation and the oceanic cycling of the organic chelators are still poorly understood. It has become increasingly recognized that a myriad of organic Fe-binding structures will coexist in oceanic waters. Recent studies also have shown that dissolved iron occurs in soluble and colloidal fractions which have important implications for the iron cycle in the ocean (Nishioka et al., 2003;

Bergquist et al., 2007; Wu et al., 2001). However, only a few studies have examined the size-spectrum of the dissolved organic ligands in oceanic waters (Wu et al., 2001; Cullen et al., 2006; Boye et al., 2005; Kondo et al., 2008). The first profiles of both soluble iron and iron binding organic ligands (<0.02 μm) from the North Atlantic and North Pacific exhibited a nutrient-like profile (Wu et al., 2001). By contrast colloidal iron (>0.02–<0.4 μm) showed a maximum at the near surface and a minimum in the nutricline in these oceanic basins where iron may be bound to organic ligands present in the colloidal size range (Wu et al., 2001). Similar distributions of soluble and colloidal ligands have been observed in the Western Atlantic basin (Cullen et al., 2006). Lately a first complete description of the physical and chemical speciation of dissolved iron and Fe-binding ligands was recorded in iron-enriched waters during a mesoscale iron enrichment in the open Southern Ocean (EISENEX) (Boye et al., 2005; Nishioka et al., 2005; Croot et al., 2005). This work showed that the added iron existed principally as colloids (>200 kDa–<0.2 μm) in the surface enriched waters (Nishioka et al., 2005) similar to the newly produced ligands (Boye et al., 2005), but the organic nature of colloidal ligands and its complexes with iron was not certain in this experiment (Boye et al., 2005). By contrast most of the increase of the dissolved Fe-binding ligands observed during a mesoscale iron enrichment

---

* Corresponding author. Tel.: +33 2 98 49 86 51; fax: +33 2 98 49 86 45.
E-mail address: marie.boye@univ-brest.fr (M. Boye).
[1] Now at Laboratoire des Sciences de l'Environnement Marin (LEMAR), CNRS UMR6539, Institut Universitaire Européen de la Mer, Technopole Brest-Iroise, 29280 Plouzane, France.
[2] Now at: Forschungsbereich Marine Biogeochemie, Chemische Ozeanographie, Leibniz-Institut für Meereswissenschaften, Dienstgebäude Westufer, Düsternbrooker Weg 20, 24105 Kiel, Germany.

experiment in the western subarctic North Pacific (SEEDS II) was attributable to the soluble fraction (Kondo et al., 2008), possibly depicting differences in ambient water-masses chemistry, physics and biological features. The discrete size classes of dissolved iron could impact the iron cycling in different ways since colloidal iron-species may be more chemically dynamic (Boye et al., 2005; Nishioka et al., 2005) hence controlling iron removal from the surface waters (Wu et al., 2001) and possibly in deep waters with implication in the inter-basin fractionation (Bergquist et al., 2007), although truly soluble iron-species may be more bio-available, controlling then the primary producers community structure (Wu et al., 2001).

Here we report the vertical distribution of size-fractionated dissolved (<0.2 μm) iron and its ligands (soluble <200 kDa, and 200 kDa<colloidal<0.2 μm) in the ambient waters of the Southern Polar Frontal Zone to investigate the size-partitioning of the so-called 'dissolved' organic iron.

2. Methods

Filtered (<0.2 μm) and ultrafiltered (<200 kDa) seawater was collected between 0 and 1000 m depth in the Atlantic sector of the Southern Ocean (along the 20–21°E meridian, between latitudes 47.7°S and 49.3°S) in late spring (November 2–25th 2000) on board of the Research Vessel *Polarstern* (cruise ANTXVIII/2, also referred as the "EISENEX" Fe-enrichment experiment). Samples were collected using acid-cleaned Teflon coated Go-Flo bottles suspended on a Kevlar wire (Croot et al., 2005). Filtered samples (<0.2 μm; Sartorius Sartobran filter capsule) were collected in low density polyethylene (LDPE) bottles for iron and the ligands determination. Additional filtrate (<0.2 μm) samples collected into acid-cleaned 500 ml polycarbonate were immediately size-fractionated by a clean inline ultrafiltration system using a 200 kDa (~0.03 μm) polyethylene hollow-fiber ultrafilter unit (Sterapore) under a laminar flow clean air hood aboard (Nishioka et al., 2005). The smaller fraction (<200 kDa) was collected in acid-cleaned low density polyethylene bottles for iron and the ligands analyses. Then for both iron and the ligands, operational definitions were taken as "dissolved" being the filtrate <0.2 μm, and "soluble" being the ultrafiltrate <200 kDa. The "colloidal" fraction was obtained as the difference calculated between these two fractions (e.g., 200 kDa <colloidal <0.2 μm). In this sampling procedure it cannot be excluded that the soluble Fe fraction may include some very small colloids (Nishioka et al., 2001; Wells et al., 1998), hence introducing underestimation of the colloidal Fe fraction. Furthermore the colloidal fractions of both iron and the ligands are estimated by difference between the analyses of the dissolved and the soluble fractions, rather than a direct measurement from the retentate of the ultrafiltration. Such procedures and calculations have been used previously to estimate colloidal Fe (Nishioka et al., 2001, 2003, 2005; Wu et al., 2001; Cullen et al., 2006; Bergquist et al., 2007) and the Fe-complexing ligands in the small size-spectrum (Wu et al., 2001; Boye et al., 2005; Cullen et al., 2006; Kondo et al., 2008).

Dissolved and soluble iron concentrations were determined as Fe(III)-species with an automatic flow injection analytical system (Kimoto Electric, Ltd.) using concentration onto an 8-hydroxyqui-noline chelating column, recovered after acidification at pH 3.2 and chemiluminescence detection (Obata et al., 1993). More recently the SAFE cruise has shown that the iron concentrations with such acidification procedure yielded slightly lower values than those after acidifying at pH less than 1.8 (Johnson et al., 2007). The method and most of the ambient size-fractionated iron concentra-tions are described in detail in Nishioka et al. (2005). The detection limit (three times the standard deviation) of Fe(III) concentrations for purified seawater (seawater passed through 8-hydroxyquinoline resin column three times) on this cruise was 15–32 pM (Nishioka et al., 2005). The relative coefficient of variation was within 5% ($n = 12$) for replicate measurements of a seawater sample contain-

ing 0.53 nM Fe(III), within 6% ($n = 9$) for 5.3 nM Fe(III) (Nishioka et al., 2005). The relative standard deviation of the filtration method with polyethylene hollow-fiber ultrafilter was 11% for replicate filtration of a seawater sample containing 0.1 nM Fe(III) and 9% for replicate filtration of a seawater sample containing 0.8 nM Fe(III). Dissolved and soluble iron concentrations were used to estimate the organic speciation in the dissolved and soluble size-fractions respectively.

The organic complexation of iron was determined aboard the ship by complexing capacity titrations in the dissolved and the soluble filtrates, using cathodic stripping voltammetry (CSV) with ligand competition against 2-(2-thiazolylazo)-*p*-cresol (TAC) (Croot and Johansson, 2000). The methodologies and procedures employed in this work are fully described in Boye et al. (2005). Briefly, 220 ml aliquot of seawater was buffered with 5 mM of borate buffer, followed by addition of 10 μM TAC. After mixing eleven 20 ml aliquots of sample were pipetted into Teflon vials spiked with increasing additions of iron. After an overnight equilibration labile iron concentrations were determined by CSV. Voltammetric conditions used were as follows: a 200 s N_2 purge; a −0.4 V adsorption potential for 200–400 s; a quiescent period of 10 s; and a fast linear sweep waveform scanning mode using a scan rate of 10 V s^{-1}. Using this procedure the detection limit (3 times the standard deviation) of the CSV iron analyses in clean seawater was 30 pM (Boye et al., 2005). The standard deviations of the ligand concentrations (L) and the conditional stability (K'_{FeIIIL}) constants were calculated from linear least-square regression of the titration curves fitted for a single ligands group (Boye et al., 2001). The relative standard deviation (precision) of repeated determinations of the ligand concentration was better than 5% and better than 1% for the conditional stability constant (Boye et al., 2005).

3. Results and discussion

3.1. Study area

The four sampling stations were geographically located within the broad eastward-flowing Antarctic Circumpolar Current (ACC) north of the Antarctic Polar Front (APF) that had its major jet centered at roughly 49°30′S (Strass et al., 2001). However, at stations 9, 48 and 91 in the latitude range 47°49′S–48°36′S a subsurface temperature minimum layer was observed at around 180–200 m depth bound by the 2 °C isotherm, characteristic of Antarctic Winter Water (Belkin and Gordon, 1996) (Figs. 1–2). Furthermore the horizontal currents measured with a VM-ADCP at these stations (Strass et al., 2001) showed vanishingly low or even westward currents. The Winter Water and current pattern indicated that the three stations were located within a cyclonic eddy, which likely had shed from the APF by detachment from a northward protruding meander (Cisewski et al., 2005). The vertical mixing in the eddy and its evolution in the course of the EISENEX experiment were well studied since the eddy served as the hydrographic structure for the three iron infusions (Cisewski et al., 2005). From the relative position of the stations and the eddy core, station 9 was located in the center of the eddy before the first iron release, station 48 was on the edge of the eddy on its southern bottleneck one day after the second Fe-release, and station 91 was sampled in the eddy on the edge of the second infused patch about ten days after the second Fe-release and about 3–4 days after a second storm had crossed the patch area. The temperature in the subsurface temperature minimum at station 7 (Figs. 1–2) was above 2 °C, related to the fact that this station was located north of the Antarctic Polar Front but outside and to the south of the eddy.

The eddy carried with it the nutrients signature of the waters originating from the southern side of the APF, with a high surface residual level of nitrate (22–24 μM) and relatively higher surface silicate levels (12–14 μM) compared to station 7 located outside of the eddy (9 μM) (Fig. 3). The mixed layer depth generally deepened with time
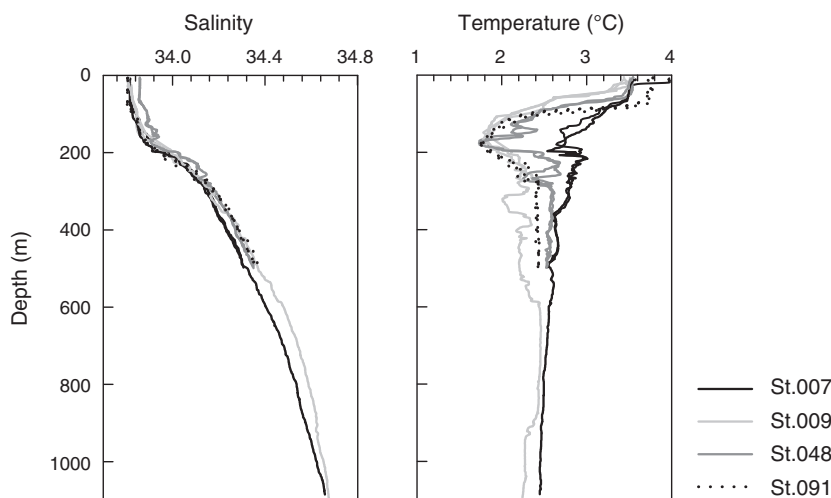
Fig. 1. Salinity and temperature profiles in the top 1100 m recorded at stations #007 (49.29°S, 20.02°E), #009 (47.82°S, 20.79°E), #048 (48.59°S, 20.72°E), and #091 (48.17°S, 21.09°E). (CTD data recording and validation as described by Strass et al., 2001.)

(~20 m at station 7, and from ~30 m at station 9 and station 48 to 90 m mixed layer depth at station 91 in the eddy; Fig. 1). Chlorophyll-*a* displayed relative concentration maxima in the upper 100 m (Fig. 3), with lower mean values outside of the eddy (e.g.; 0.33 µg l^{-1} at station 7) compared to inside the eddy (e.g.; 0.52 µg l^{-1} at station 9 and 0.73 µg l^{-1} at station 91) and on its edge (e.g.; 0.54 µg l^{-1} at station 48) (Gervais et al., 2002). The pico- (<2 µm) and nano-phytoplankton (2–20 µm) dominated the phytoplankton assemblage in these waters accounting for 28–39% and 42–52% of Chl-*a* respectively (Gervais et al., 2002).

The chlorophyll-*a* levels at stations located inside the Fe-patch after the second infusion, immediately prior to sampling the out-patch stations, displayed much higher mean concentrations (e.g., 1.26 µg l^{-1} at station 46, and 1.64 µg l^{-1} at station 88) compared to station 48 (0.55 µg l^{-1}) and station 91 (0.73 µg l^{-1}), respectively. No storm or precipitation events occurred between the respective in- and out-patch stations that could have caused a dilution of the Fe-fertilized water characteristics. This suggests that the top 200 m of stations 48 and 91 was unlikely imprinted by the biogeochemical signals of the second iron infusion, hence they featured the eddy waters that originated from the southern side of the Antarctic Polar Front as for station 9.

3.2. The size-spectrum of dissolved iron

The ultrafiltration procedure of soluble iron and the calculation mode of colloidal iron may have introduced sampling bias since
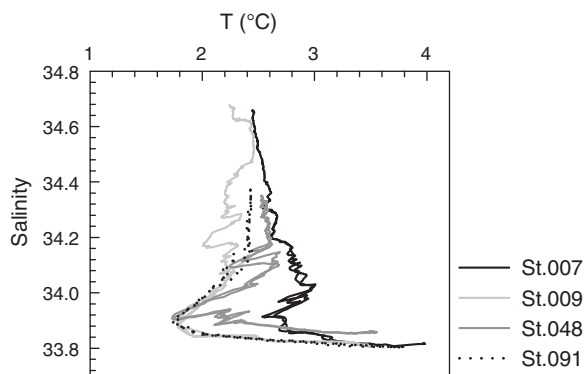

Fig. 2. Temperature–salinity diagram in the top 1100 m at stations #007 (49.29°S, 20.02°E), #009 (47.82°S, 20.79°E), #048 (48.59°S, 20.72°E), #091 (48.17°S, 21.09°E). (CTD data recording and validation as described by Strass et al., 2001.)

colloidal Fe could be formed or adsorbed onto the filter during the ultrafiltration step or on the contrary could solubilize. Comparisons between microfiltration methods and cross flow filtration (using the method described in Wen et al., 2000) however did not show any significant difference in the colloidal Fe concentrations even at low levels such as 90 pM (Wu et al., 2001), indicating that colloidal Fe based on the difference of Fe concentrations analysed in the dissolved and soluble fractions is likely due to particulate retention rather than Fe adsorption/desorption by the ultrafilter (Wu et al., 2001). Good mass balances for Fe were also obtained using a cross flow filtration system employed with a 10 kDa membrane in typical oceanic waters (Schlosser and Croot, 2008). The colloidal Fe concentrations calculated here as the difference between the dissolved and soluble fractions are 2–12 and 3–25 times higher than the 5% precision of dissolved Fe and soluble Fe concentrations, respectively (Table 1), suggesting good reliability of the estimation of the colloidal fraction. Furthermore paired two-tailed *t*-test shows that the differences between dissolved and soluble Fe, equivalent to colloidal Fe, are statistically significant at the 95% confident interval ($P = 0.05$, $t_{critical} = 1.72$, $t_{experimental} = 4.45$, $n = 22$).

Dissolved Fe and soluble Fe roughly exhibit nutrient-like profiles (Fig. 4), with depleted concentrations in surface waters (mean values respectively, 65 ± 18, 43 ± 14 pM) and increasing concentrations in deeper waters below the Antarctic Winter Water (230 ± 100, 130 ± 40 pM respectively). Colloidal Fe concentrations are much lower in surface waters (mean value, 23 ± 9 pM) compared to soluble Fe suggesting that colloidal iron may be more efficiently removed from surface waters than soluble iron (Fig. 4). In deeper waters colloidal iron gradually increases (mean value, 100 ± 60 pM) (Fig. 4). Despite station 7 being located outside of the eddy, the two data points gathered at 50 m and 1000 m at this station are in the same range than the concentrations recorded at the other stations, located within the eddy (Table 1). The data indicate that dissolved Fe is principally present in the soluble size range in the surface waters (accounting for 63 ± 8% of dissolved Fe), while in deeper waters below 500 m the colloidal and soluble Fe portions of dissolved Fe are almost equally balanced (51 and 49% respectively). Based on molecular diffusion rate of spherical species through liquid that is inversely related to their radius (Einstein–Stokes relation), soluble Fe (size <~30 nm) should be more available for phytoplankton uptake than colloidal Fe species (diameters ~30–200 nm), provided the uptake is limited solely by diffusion of Fe species to the cell surface. Furthermore diffusion limitation increases markedly with increasing cells size or cells-aggregates size (Timmermans et al., 2004). Diffusion limitation may
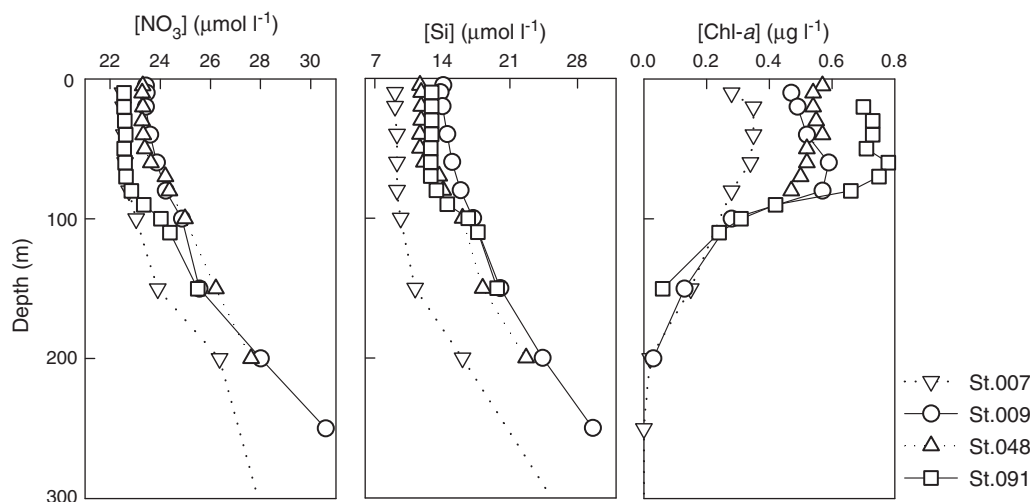
Fig. 3. Nitrate, silicate (Hartmann et al., 2001; Kattner, 2009) and chlorophyll-*a* (Riebesell et al., 2001) concentrations in the top 300 m at stations #007 (49.29°S, 20.02°E), #009 (47.82°S, 20.79°E), #048 (48.59°S, 20.72°E), and #091 (48.17°S, 21.09°E).

thus be less severe for pico- and nano-phytoplankton that dominate the phytoplankton assemblage in these waters (Gervais et al., 2002) than for other typical austral large (chain-forming) diatom species like *Fragilariopsis kerguelensis* (individual cells 60 μm long, 20 μm wide). In turn biological uptake of soluble Fe by the smallest phytoplankton combined with low Fe inputs in the surface waters, and possibly aggregation and settling or particles scavenging of colloidal iron similar to Th isotopes (Savoye et al., 2006), accompanied by the releases of both soluble and colloidal Fe in the twilight zone by remineralisation of sinking particles and by desorption hence could create the dissolved Fe profiles observed in these polar waters (Fig. 4).

Despite lower abundance, colloidal Fe still comprised ~37% of the dissolved Fe fraction in the surface waters. This value is slightly higher than in surface layers of the subarctic (~23%) and equatorial (~15%) Pacific (Nishioka et al., 2001, 2003; Wells, 2003), but substantially lower than what is reported for the near-surface waters of the north Atlantic and Pacific (80–90%) (Wu et al., 2001), for the surface waters of the north western Atlantic (65–90%) (Cullen et al., 2006), and for artificially Fe-enriched surface waters of the austral PFZ (~76%) (Nishioka et al., 2005) and of the northwestern subarctic Pacific (~64%) (Kondo et al., 2008). Differences in fractionation methodologies can cause these differences (Wells, 2003). It is also likely that the different Fe supplies (e.g., atmospheric sources, upwelling, artificial Fe supply, and lithogenic sources) in these areas can influence the colloidal Fe percentage (Nishioka et al., 2005).

3.3. The size-spectrum of dissolved ligands

The colloidal ligand concentrations calculated as the difference between the dissolved and soluble fractions are occasionally within (at three surface waters data points), but mostly well above (by 2 to 11 times), the 5% precision of dissolved L and soluble L concentrations (Table 1), suggesting that these values are not artifacts of the calculation method. The paired two-tailed *t*-test also shows that the differences between dissolved and soluble L (e.g., equivalent to colloidal L) are statistically significant at the 95% confident interval ($P = 0.05$, $t_{\text{critical}} = 1.73$, $t_{\text{experimental}} = 7.48$, $n = 20$). Furthermore the data points recorded at station 7 located outside of the eddy compared well with the ligands concentrations observed at similar depths in the eddy (Table 1).

Dissolved L and soluble L distributions suggest a biological source in surface waters with relative maxima at the base of the chlorophyll-*a* rich layer (maximum value, 0.9 nM, 0.8 nM, respectively), and a fairly constant distribution in deeper waters (mean values of 0.70 ± 0.07 and

0.50 ± 0.05 nM respectively) (Fig. 5). The two samples taken at 300 and 400 m depth at station 9 however deviate somewhat from this generally homogenous distribution in that soluble ligand here makes a comparably higher contribution to the dissolved ligand pool, and is probably related to the fact that station 9 in the center of the eddy features also the coldest water in that depth range, e.g., water from the most southerly origin (Fig. 1). By contrast iron-complexing colloids do not show a maximum in surface waters, but its concentration gradually increases with depth in the mesopelagic zone (from minimal values of 0.06 ± 0.02 nM in surface waters up to 0.15 ± 0.06 nM below the Antarctic Winter Water core) (Fig. 5). Thereby the vertical distribution of Fe-complexing colloids is possibly driven by its aggregation and settling and/or its particle scavenging (adsorption to and removal on sinking particles) from the upper ocean, and its release in deeper waters by remineralisation, disaggregation and by desorption from particles. The data indicate that dissolved ligands are mainly present in the soluble size range in the surface waters (representing $91 \pm 2\%$ of dissolved L), although iron-complexing colloids abundance increases significantly in deeper waters (accounting for 13–35% of the dissolved pool below 200 m, compared to 4–12% in the surface layer). Consequently the ratio $[L_{\text{sol}}]/[L_{\text{coll}}]$ is much higher in surface waters (~13) compared to deeper waters below 200 m (~4). Biological production of soluble ligands in surface waters and removal of iron-complexing colloids from the upper layer may hence drive the distribution of dissolved ligands in these waters. In deeper waters regeneration of sinking material, bacterial decomposition and possibly desorption from particles may supply relatively more colloids compared to soluble ligands. Regeneration of sinking biogenic particulate organic material is thought to be an important source for soluble L in the north Atlantic and Pacific (Wu et al., 2001).

No significant difference in the conditional stability constant of dissolved iron complexes ($\text{LogK}'_{\text{FeL-diss}}$) was depicted between the surface (~21.95) and the deeper waters (~21.98) (Table 1), and only a single ligand group was evident from the resolution of the titration curves of the dissolved ligands by applying the linear least-squares regressions. It means that the small size-spectrum could not be resolved by applying CSV titration method in the dissolved fraction alone, and that ultrafiltration is required to discriminate the ligands by size.

3.4. The complexation of dissolved iron in the small size-fractions

Soluble and colloidal Fe may be present principally bound to soluble ligands and colloidal ligands respectively. Soluble L are indeed

Table 1

Concentrations of iron and Fe-binding ligands measured in the dissolved (<0.2 µm) and soluble (<200 kDa) fractions at 4 stations in the Southern Ocean during the ANTXVIII/2 (EISENEX) expedition. The colloidal iron and ligand concentrations were calculated as the difference between the dissolved (<0.2 µm) and the soluble (<200 kDa) fractions. The standard deviation of iron (sdv) was calculated using the relative coefficient of variation of the measurement (equal to 5%; see text). The conditional stability constants of the iron(III)–ligand complexes (LogK′) were calculated by linear least-squares regression of the titration fitted for a linear equation (Ruzic, 1982). The standard deviations (sdv) of the ligands and LogK′ were calculated from linear least-squares regression of the titration curves fitted for a single ligands group (Boye et al., 2001). The fraction of soluble iron was calculated with the iron analyses ($Fe_{sol}/Fe_{diss\ measured}$) and compared to the ratio predicted from the thermodynamic model ($Fe_{sol}/Fe_{diss\ from\ model}$; calculated using Eq. (1); see text). The error on ($Fe_{sol}/Fe_{diss)from\ model}$ was calculated as equal to $(Fe_{sol}/Fe_{diss})_{from\ model} * \sqrt{[(Ln(10)*sdvLogK'_{sol})^2 + (Ln(10)*sdvLogK'_{diss})^2 + (sdvSol\text{-}Fe/Sol\text{-}Fe)^2 + (sdvDiss\text{-}Fe/Diss\text{-}Fe)^2]}$. The physical partitioning of iron into soluble and colloidal size-fractions can be further estimated by subtracting the ratio Fe_{sol}/Fe_{diss} to 1 to obtain the fraction of colloidal iron.

Station no. / Position / Date	Depth (m)	Dissolved Fe (nM)	Sdv diss Fe (nM)	Soluble Fe (nM)	Sdv sol Fe (nM)	Colloidal Fe (nM)	Dissolved L (nM)	Sdv diss. L	LogK′diss.	Sdv LogK′diss.	Soluble L (nM)	Sdv sol. L	LogK′sol.	Sdv LogK′sol.	Colloidal L (nM)	$(Fe_{sol}/Fe_{diss})_{measured}$	$(Fe_{sol}/Fe_{diss})_{from\ model}$	Err. $(Fe_{sol}/Fe_{diss})_{from\ model}$ (rsd)
St.007 49.29°S 20.02°E 02/11/00	50	0.05	0.0025	0.03	0.0015	0.03	0.71	0.05	22.34	0.47	0.63	0.04	21.56	0.1	0.08	0.60	0.15	0.17
	1000	0.39	0.0195	0.18	0.009	0.21	0.85	0.04	22.58	0.54	0.59	0.06	21.85	0.28	0.26	0.46	0.17	0.23
St.009 47.82°S 20.79°E 07/11/00	20	0.08	0.004	0.05	0.0025	0.03	0.58	0.01	22.04	0.13	0.53	0.09	22.15	0.61	0.05	0.63	1.24	1.79
	40	0.06	0.003	0.03	0.0015	0.03	0.61	0.09	21.56	0.28	0.54	0.06	21.59	0.12	0.07	0.50	0.99	0.72
	60	0.04	0.002	0.03	0.0015	0.01	0.74	0.03	22.03	0.19	0.7	0.11	21.55	0.19	0.04	0.75	0.32	0.20
	80	0.07	0.0035	0.04	0.002	0.03	0.76	0.04	22.32	0.35	0.68	0.05	21.64	0.14	0.08	0.57	0.19	0.17
	200	0.1	0.005	0.08	0.004	0.02	0.62	0.05	22.18	0.41	0.53	0.03	21.89	0.21	0.09	0.80	0.44	0.47
	250	0.14	0.007	0.08	0.004	0.06	0.64	0.05	22.16	0.38	0.51	0.06	21.31	0.07	0.13	0.57	0.12	0.11
	300	0.16	0.008	0.13	0.0065	0.03	0.75	0.06	22.01	0.27	0.64	0.05	22.1	0.32	0.11	0.81	1.06	1.03
	400	0.2	0.01	0.17	0.0085	0.03	0.8	0.07	22.04	0.33	0.69	0.03	21.8	0.13	0.10	0.85	0.50	0.41
St.048 48.59°S 20.72°E 17/11/00	20	0.05	0.0025	0.03	0.0015	0.02	0.63	0.04	21.59	0.16	0.59	0.02	22.63	0.82	0.03	0.60	10.54	20.30
	40	0.04	0.002	0.03	0.0015	0.01	0.65	0.1	22.86	1.19	0.62	0.02	22.39	0.61	0.03	0.75	0.33	1.01
	60	0.06	0.003	0.04	0.002	0.02	0.76	0.04	21.98	0.2	n.a.	–	n.a.	–	–	0.67	–	–
	80	0.09	0.0045	0.08	0.004	0.01	0.78	0.22	21	0.03	n.a.	–	n.a.	–	–	0.89	–	–
	100	n.a.	–	0.08	0.004	–	n.a.	–	n.a.	–	0.59	0.1	21.44	0.15	–	–	–	–
St.091 48.17°S 21.09°E 25/11/00	50	0.11	0.0055	0.07	0.0035	0.04	0.86	0.08	21.74	0.19	0.76	0.05	21.66	0.12	0.1	0.64	0.77	0.41
	200	0.07	0.0035	0.05	0.0025	0.02	0.68	0.05	22.59	0.6	0.57	0.09	21.25	0.09	0.11	0.71	0.04	0.06
	300	0.18	0.009	0.11	0.0055	0.07	0.6	0.08	21.32	0.06	0.46	0.05	22.84	0.79	0.14	0.61	27.29	50.01
	400	0.18	0.009	0.12	0.006	0.06	0.63	0.06	21.6	0.15	0.54	0.02	22.9	0.72	0.09	0.67	18.52	31.43
	500	0.26	0.013	0.15	0.0075	0.11	0.66	0.09	21.5	0.16	0.55	0.05	22.46	0.62	0.11	0.58	9.06	13.43
	600	0.35	0.0175	0.19	0.0095	0.16	0.69	0.07	21.63	0.17	0.49	0.02	22.25	0.32	0.2	0.54	3.66	3.08
	800	0.34	0.017	0.15	0.0075	0.19	0.65	0.05	21.63	0.14	0.42	0.05	21.86	0.32	0.23	0.44	1.48	1.20
	1000	0.41	0.0205	0.21	0.0105	0.2	0.78	0.05	22.51	0.54	0.52	0.03	22.38	0.43	0.26	0.51	0.62	0.99

n.a. means not analysed.

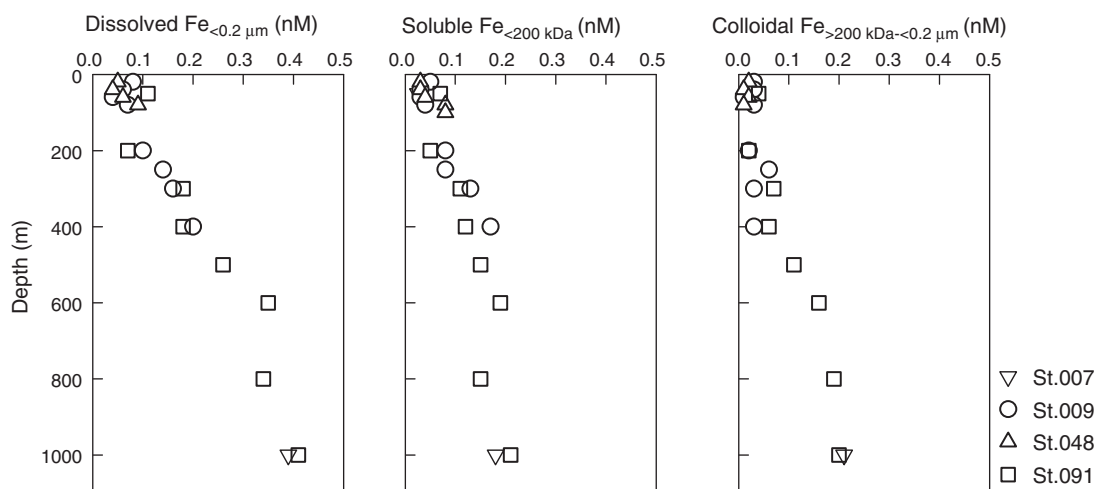**Fig. 4.** Vertical profiles of iron measured in the dissolved (<0.2 μm) and soluble (<200 kDa) fractions, and calculated in the colloidal fraction (>200 kDa–<0.2 μm) for stations #007 (49.29°S, 20.02°E), #009 (47.82°S, 20.79°E), #048 (48.59°S, 20.72°E), and #091 (48.17°S, 21.09°E) in the Southern Ocean.

in excess over soluble Fe by ~0.5 nM on average (Table 1; Fig. 6), while colloidal L are comparatively almost saturated in colloidal Fe providing the relationship between the two parameters is linear with a slope almost equal to 1 (e.g.; $[Fe_{coll}] = 0.90 [L_{coll}] - 0.04$ nM, $r^2 = 0.88$, $n = 20$; Fig. 6). The largest saturation of colloids with Fe and the excess of soluble L over soluble Fe are obtained at the thermodynamic equilibrium in these waters. Hence it suggests that soluble ligands have the potential to buffer an iron input to surface waters whereas colloidal iron complexes may aggregate and settle.

Soluble Fe exists mainly as organic soluble complexes but it was not possible to discern whether iron colloids (e.g., the colloidal iron complexes) exist as organic complexes and/or inorganic amorphous colloids from the data. Recent findings suggest that humic substances (HS) may account for a major portion of Fe complexation in seawater and that a fraction of the Fe-HS species has a colloidal behavior (Laglera and van den Berg, 2009). It is hence conceivable that the extremely low concentration of free colloidal iron-complexing sites (e.g., 0–80 pM) is related to few complexation sites embedded within an intricate architecture of very large molecular condensates. On the other hand inorganic Fe colloids can form surface active amorphous colloids (Wells, 2003) that may appear as a (saturated) strong Fe-binding capacity upon titration (Boye et al., 2005), and/or provide a linear relationship between colloidal Fe and iron-complexing colloids with a slope nearly equal to 1 like in this study. For instance

comparison between simple models of dissolved Fe equilibrium portioning and iron measurements in the dissolved and soluble fractions suggested an inert colloidal fraction in the northwestern Atlantic that could be an iron oxide (Cullen et al., 2006). To assess such possibility we developed a model of iron portioning between soluble and colloidal fractions, resting on the relationship: FeL/Fe′ = K′$_{FeL}$*L′, which is obtained at the equilibrium of Fe′ + L′ ←→ FeL. In this relationship, FeL is the concentration of the organic iron, Fe′ the concentration of inorganic iron, L′ the concentration of excess ligands (e.g., not bound to iron) and K′$_{Fe′L}$ the conditional stability constant of Fe–L complexes. Then the following Eq. (1) was obtained to predict the ratio of Fe$_{sol}$/Fe$_{diss}$ at the thermodynamic equilibrium, by using the relationship in the soluble and dissolved iron fractions, and by assuming Fe′$_{sol}$ ≈ Fe′$_{diss}$ (Fig. 6):

$$(Fe_{sol}/Fe_{diss})_{from\ model} = (1 + L'_{sol}*K'_{FeL-sol})/(1 + L'_{diss}*K'_{FeL-diss}) \quad (1)$$

The fraction of soluble iron predicted from the thermodynamic model (Fe$_{sol}$/Fe$_{diss\ from\ model}$) did not show however any significant trend with the ratio calculated from the iron analyses (Fe$_{sol}$/Fe$_{diss\ measured}$) in these waters (Table 1). Conversely, a systematically lower proportion of soluble iron was estimated from the model compared to the measurements in the North Atlantic (Cullen et al., 2006). The ratio estimated from our model even displayed some values far above 1, with large
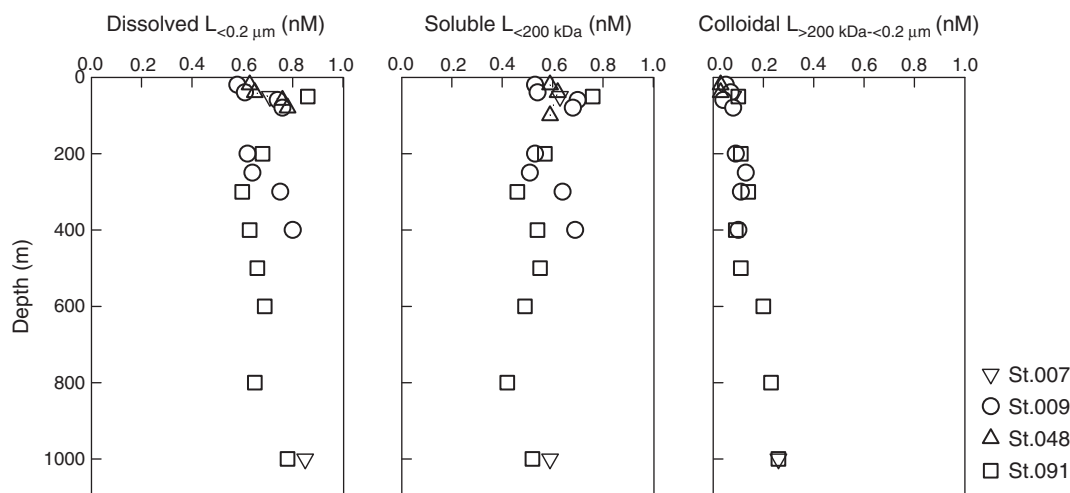

Fig. 5. Vertical profiles of the iron binding ligand measured in the dissolved (<0.2 μm) and soluble (<200 kDa) fractions, and calculated in the colloidal fraction (>200 kDa–<0.2 μm) for stations #007 (49.29°S, 20.02°E), #009 (47.82°S, 20.79°E), #048 (48.59°S, 20.72°E), and #091 (48.17°S, 21.09°E) in the Southern Ocean.
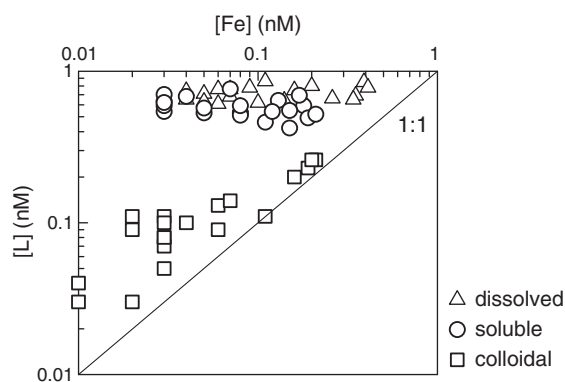
Fig. 6. Relationships between iron and ligand in the dissolved (triangles), soluble (circles) and colloidal (squares) fractions using all data obtained throughout the 0–1000 m water column at the stations #007, #009, #048, and #091.

uncertainties (Table 1). This is likely generated by the difference between the fractions being at the same scale as the analytical detection limits and errors in these waters, and because the colloidal component was very small in the Southern Ocean compared to the North Atlantic (Cullen et al., 2006). Colloidal iron complexes still account for ~37% on average of the operationally defined dissolved organic iron in the surface waters of the Southern Ocean, and up to 51% on average below 500 m depth. Furthermore the calculations of ligand excess over iron indicate that the colloidal binding-sites are the most saturated with Fe (e.g., the concentration of free colloidal iron-complexing sites is <80 pM) compared with the soluble ligands (e.g., soluble L are in excess over soluble Fe by about 500 pM), and that any extra Fe inputs would bind to soluble ligands. Artificial Fe-enrichment conducted in this area conversely shows that more iron-complexing colloids are quickly produced in response to the Fe-fertilization and that most of the infused Fe is present in the colloidal size range (Boye et al., 2005; Nishioka et al., 2005). However such Fe-infusion experiments may not reflect the chemical and physical responses of the iron cycle to natural Fe enrichments (Boye et al., 2005). For instance it is not possible to say if the iron-complexing colloids produced after an artificial Fe addition (Boye et al., 2005) were of the same chemical nature as the colloids naturally present in the oceanic waters.

Using the concentrations of iron and ligands in the soluble and colloidal fractions, and the stability constants of soluble Fe complexes in the equation given by Wu et al. (2001); e.g., $K'_{FeL-sol}/K'_{FeL-coll} = (Fe_{sol}/Fe_{coll}) \cdot (L_{coll}/L_{sol})$, the ratios of the stability constants of soluble complexes to iron colloids ($K'_{FeL-sol}/K'_{FeL-coll}$) are calculated to be <1 at all depths. These calculations suggest that iron-complexing colloids have a higher stability constant for binding Fe compared to the soluble ligands (mean $LogK'_{FeL}$ values of 22.5 ± 0.4 and 21.9 ± 0.4 respectively) similar to the observations in the Fe-enriched surface waters of the northwestern subarctic Pacific (Kondo et al., 2008). The opposite tendency is found in deep waters of the North Pacific (Wu et al., 2001), possibly depicting different ligands in deep waters of different oceans. The difference in stability constant between soluble and colloidal fractions is obviously not high enough (being in the range of stability constants of dissolved complexes observed previously in the Southern Ocean; Boye et al., 2001) to either explain why soluble free ligands are in excess (e.g., by ~500 pM) or why there is little of free colloidal iron-complexing sites (e.g., <80 pM). The difference in stability constant indicates however that soluble Fe complexes should be more readily exchangeable buffering of Fe′ (e.g., the free inorganic iron) compared to strong Fe colloids. It fits with results resting on thermodynamic model assessed for the northwest Atlantic (Cullen et al., 2006). At the thermodynamic equilibrium, our data also show that Fe-complexing colloids are the most saturated with iron (Fig. 6) while the exchangeable fraction for Fe uptake through Fe complexes dissociation (e.g., without photochemistry) occurs in the soluble

fraction. In turn both the speciation of Fe at equilibrium and the stability constant implicate that Fe bound to soluble ligands may be more available for uptake by phytoplankton than Fe bound to colloids, provided that Fe′ that easily dissociates from the weaker soluble complexes is available directly or indirectly through its reduction at the cell surface (Shaked et al., 2005). It is also possible that both soluble and colloidal Fe complexes supply bio-available free inorganic iron (as Fe(III) or Fe(II)) through photo-reduction of the complexes or via reduction at the cell surface (Shaked et al., 2005), but the concentration of Fe′ (or Fe(II)) produced from the colloidal Fe complexes through these processes would be so low that it may not sustain Fe requirement of any cells. So following the more recent model of Fe uptake (Shaked et al., 2005) colloidal Fe complexes unlikely represent a significant pathway for iron uptake in these waters. The higher bio-availability of soluble Fe would be also in line with expectations based on the Fe diffusion rates. The calculations also imply that Fe strongly bound to colloids could be scavenged more efficiently than soluble iron. However the colloidal ligands may not have a large extra capacity to remove iron from the water column since there is little of free-iron colloids. Processes of Fe removal in deep waters, including aggregation of colloids and settling, are deemed to control the dissolved iron concentration in deep waters (Wu et al., 2001; Bergquist et al., 2007). The presence of transparent exopolymer particles (TEP) in seawater (Passow, 2002) may play an important role in the processes of iron scavenging. For instance the TEP-precursors, mainly acidic polysaccharide fibrils, released by phytoplankton and especially by diatoms as well as by bacteria are in the colloidal size range (>1 kDa) (Passow, 2000) and might be good Fe-binding ligands (Buffle et al., 1998). Complexation with polysaccharides is further suggested by the increase of the partition coefficient for Fe in polysaccharides-enriched fractions of colloidal organic matter (Quigley et al., 2002). Coagulation of colloidal TEP-precursors may form submicron aggregates that behave like particles (Buffle et al., 1998), hence resulting in a major route for scavenging of Fe bound to these precursors. Surface active substances that may be TEP-precursors (Passow, 2000) were actually found to accumulate in surface Fe-enriched waters in the Southern Ocean during the EIFEX experiment as the diatoms induced bloom developed (Croot et al., 2007), concomitantly with a loss of colloidal and particulate iron. The distribution of colloidal Fe and iron-complexing colloids observed in our study suggests a possible aggregation and settling and/or particles scavenging of Fe colloids in surface waters similar to Th isotopes (Savoye et al., 2006), and its release in deeper waters by remineralisation, disaggregation and by desorption from particles. This provides a pathway for export of colloidal Fe complexes through TEP aggregates and their settling from surface waters, and their breakup in deeper waters, while it keeps the possibility of colloidal Fe complexes to be inorganic colloids as well following similar processes including desorption from particles in deep waters. TEP has been also studied as a binding ligand of thorium (Santschi et al., 2006; Passow et al., 2006), and polysaccharides-enriched fractions of the colloidal organic matter were found to display the highest partition coefficient of any known marine mineral sorbent for ^{234}Th (Quigley et al., 2002). Hence Th isotopes might provide some useful information on iron complexation of TEP and colloidal TEP-precursors, as well as on abiotic processes governing the iron cycle in the ocean such as particles scavenging and colloids aggregation, and on its boundary scavenging. On the other hand the rather small difference in the $[Fe_{sol}]/[Fe_{coll}]$ ratio with depth suggests that some thermodynamically driven process may be buffering a relationship between soluble iron complexes and iron colloids. For example if one accepts the possibility that the molecular hydrophilicity of the soluble ligand decreases upon Fe complexation, there may be a thermodynamically driven process by which soluble ligands aggregate "hydrophobically" to form colloidal particles once Fe is complexed (perhaps more appropriately, the resistance to aggregation decreases). That could explain that there

is little of free colloidal Fe-complexing sites and it might provide an explanation for the comparatively small difference in the partitioning of iron into colloidal particles with depth. However unlike microgels, any hydrophobically-driven aggregates would not disaggregate at depth without there first being a loss of Fe from the complex, perhaps a difficult step; whereas aggregates may still be released from remineralisation of larger particles. In turn the molecular nature of iron colloids and the dynamics of the smaller fractions of dissolved iron clearly need to be further assessed. The role of soluble and colloidal iron-species also needs to be further considered in models of Fe oceanic cycling.

Acknowledgements

References

Belkin, I.M., Gordon, A.L., 1996. Southern Ocean fronts from the Greenwich meridian to Tasmania. Journal of Geophysical Research Oceans 101, 3675–3696.

Bergquist, B.A., Wu, J., Boyle, E.A., 2007. Variability in oceanic dissolved iron is dominated by the colloidal fraction. Geochimica et Cosmochimica Acta 71, 2960–2974.

Boye, M., van den Berg, C.M.G., de Jong, J.T.M., Leach, H., Croot, P., de Baar, H.J.W., 2001. Organic complexation of iron in the Southern Ocean. Deep-Sea Research I 48, 1477–1497.

Boye, M., Nishioka, J., Croot, P.L., Laan, P., Timmermans, K.R., de Baar, H.J.W., 2005. Major deviations of iron complexation during 22 days of a mesoscale iron enrichment in the open Southern Ocean. Marine Chemistry 96, 257–271.

Buffle, J., Wilkinson, K.J., Stoll, S., Filella, M., Zhang, J., 1998. A generalized description of aquatic colloids interactions: the three-colloidal component approach. Environmental Science and Technology 32, 2887–2899.

Cisewski, B., Strass, V.H., Prandke, H., 2005. Upper-ocean vertical mixing in the Antarctic Polar Front Zone. Deep Sea Research II 52, 1087–1108.

Croot, P.L., Johansson, M., 2000. Determination of iron speciation by cathodic stripping voltammetry in seawater using the competing ligand 2-(2-Thiazolylazo)-p-cresol (TAC). Electroanalysis 12 (8), 565–576.

Croot, P.L., Laan, P., Nishioka, J., Strass, V., Cisewski, B., Boye, M., Timmermans, K.R., Bellerby, R.G., Goldson, L., Nightingale, P., de Baar, H.J.W., 2005. Spatial and temporal distribution of Fe(II) and H₂O₂ during EisenEx, an open ocean mescoscale iron enrichment. Marine Chemistry 95, 65–88.

Croot, P.L., Passow, U., Assmy, P., Jansen, S., Strass, V.H., 2007. Surface active substances in the upper water column during a Southern Ocean Iron Fertilization Experiment (EIFEX). Geophysical Research Letters 34. doi:10.1029/2006GL028080.

Cullen, J.T., Bergquist, B.A., Moffett, J.W., 2006. Thermodynamic characterization of the partitioning of iron between soluble and colloidal species in the Atlantic Ocean. Marine Chemistry 98, 295–303.

Gervais, F., Riebesell, U., Gorbunov, M.Y., 2002. Changes in primary productivity and chlorophyll-a in response to iron fertilization in the Southern Polar Frontal Zone. Limnology & Oceanography 47 (5), 1324–1335.

Gledhill, M., van den Berg, C.M.G., 1994. Determination of complexation of iron III with natural organic complexing ligands in sea water using cathodic stripping voltammetry. Marine Chemistry 47, 41–54.

Hartmann, C., Richter, K.-U., Harms, C., 2001. Distribution of nutrients during the Iron experiment. Ber. Polarforsch. Meeresforsch., 400, Alfred-Wegener-Institut für Polar und Meeresforschung, Bremerhaven, Germany, pp. 186–190.

Hutchins, D.A., Witter, A.E., Butler, A., Luther III, G.W., 1999. Competition among marine phytoplankton for different chelated iron species. Nature 400, 858–861.

Johnson, K.S., Boyle, E., Bruland, K., Coale, K., Measures, C., Moffett, J., Aguilar-Islas, A., Barbeau, K., Bergquist, B., Bowie, A., Buck, K., Cai, Y., Chase, Z., Cullen, J., Doi, Y., Elrod, V., Fitzwater, S., Gordon, M., King, A., Laan, P., Laglera-Baquer, L., Landing, W., Lohan, M., Mendez, J., Milne, A., Obata, H., Ossiander, L., Plant, J., Sarthou, G.,

Sedwick, P., Smith, G.J., Sohst, B., Tanner, S., van den Berg, C.M.G., Wu, J., 2007. Developing standards for dissolved iron in seawater. EOS 88 (11), 131–132.

Kattner, G., 2009. Nutrients measured on water bottle samples during POLARSTERN Leg ANT-XVIII/2. doi:10.1594/PANGAEA.713703.

Kondo, Y., Takeda, S., Nishioka, J., Obata, H., Furuya, K., Johnson, W.K., Wong, C.S., 2008. Organic iron(III) complexing ligands during an iron enrichment experiment in the western subarctic North Pacific. Geophysical Research Letters 35, L12601. doi:10.1029/2008GL033354.

Laglera, L.M., van den Berg, C.M.G., 2009. Evidence for the geochemical control of iron by humic substances in seawater. Limnology & Oceanography 54 (2), 610–619.

Nishioka, J., Takeda, S., Wong, C.S., 2001. Change in the concentrations of iron in different size fractions during a phytoplankton bloom in controlled ecosystem enclosures. Journal of Experimental Marine Biology and Ecology 258, 237–255.

Nishioka, J., Takeda, S., Kudo, I., Tsumune, D., Yoshimura, T., Kuma, K., Tsuda, A., 2003. Size-fractionated iron distributions and iron-limitation processes in the subarctic NW Pacific. Geophysical Research Letters 30 (14), 1730.

Nishioka, J., Takeda, S., de Baar, H.J.W., Croot, P.L., Boye, M., Laan, P., Timmermans, K.R., 2005. Changes in the concentration of iron in different size fractions during an iron enrichment experiment in the open Southern Ocean. Marine Chemistry 95, 51–63.

Obata, H., Karatani, H., Nakayama, E., 1993. Automated determination of iron in seawater by chelating resin concentration and chemiluminescence detection. Analytical Chemistry 65, 1524–1528.

Passow, U., 2000. Formation of Transparent Exopolymer Particles, TEP, from dissolved precursors material. Marine Ecology Progress Series 192, 1–11.

Passow, U., 2002. Transparent exopolymer particles (TEP) in aquatic environments. Progress in Oceanography 55, 287–333.

Passow, U., Dunne, J., Murray, J.W., Balistrieri, L., Alldredge, A.L., 2006. Organic carbon to ²³⁴Th ratios of marine organic matter. Marine Chemistry 100, 323–336.

Quigley, M.S., Santschi, P.H., Hung, C.-C, Guo, L., Honeyman, B.D., 2002. Importance of acid polysaccharides for 234Th complexation to marine organic matter. Limnology and Oceanography 47, 367–377.

Riebesel, U., Gervais, F., Benthien, A., Terbrüggen, A., Schneider, A., Luz, B., Barkan, E., Altabet, M., Saunders, R., 2001. Chlorophyll-a, particulate and dissolved organic matter, primary production and stable isotope composition of POM and phytoplankton over the course of the iron fertilisation experiment. Ber. Polarforsch. Meeresforsch., 400, Alfred-Wegener-Institut für Polar und Meeresforschung, Bremerhaven, Germany, pp. 191–199.

Rue, E.L., Bruland, K.W., 1995. Complexation of iron (III) by natural organic ligands in the Central North Pacific as determined by a new competitive ligand equilibration/ adsorptive cathodic stripping voltammetric method. Marine Chemistry 50, 117–138.

Ruzic, I., 1982. Theoretical aspects of the direct titration of natural waters and its information yield for trace metal speciation. Analytica Chimica Acta 140, 99–113.

Santschi, P.H., Murray, J.W., Baskaran, M., Benitez-Nelson, C.R., Guo, L.D., Hung, C.-C., Lamborg, C., Moran, S.B., Passow, U., Roy-Barman, M., 2006. Thorium speciation in seawater. Marine Chemistry 100, 250–268.

Savoye, N., Benitez-Nelson, C., Burd, A.B., Cochran, J.K., Charette, M., Buesseler, K.O., Jackson, G.A., Roy-Barman, M., Schmidt, S., Elskens, M., 2006. ²³⁴Th sorption and export models in the water column: a review. Marine Chemistry 100, 234–249.

Schlosser, C., Croot, P.L., 2008. Application of cross-flow filtration for determining the solubility of iron species in open ocean seawater. Limnology & Oceanography: Methods 6, 630–642.

Shaked, Y., Kustka, A.B., Morel, F.M.M., 2005. A general model for iron acquisition by eukaryotic phytoplankton. Limnology and Oceanography 50, 872–882.

Strass, V.H., Leach, H., Cisewski, B., Gonzales, S., Post, J., da Silva Duarte, V., Trumm, F., 2001. The physical setting of the Southern Ocean iron fertilisation experiment. Ber. Polarforsch. Meeresforsch., 400, Alfred-Wegener-Institut für Polar und Meeresforschung, Bremerhaven, Germany, pp. 94–131.

Timmermans, K.R., van der Wagt, B., de Baar, H.J.W., 2004. Growth rates, half-saturation constants, and silicate, nitrate, and phosphate depletion in relation to iron availability of four large, open-ocean diatoms from the Southern Ocean. Limnology & Oceanography 49 (6), 2141–2151.

van den Berg, C.M.G., 1995. Evidence for organic complexation of iron in seawater. Marine Chemistry 50, 139–157.

Wells, M.L., 2003. The level of iron enrichment required to initiate diatom blooms in HNLC waters. Marine Chemistry 82, 101–114.

Wells, M.L., Kozelka, P.B., Bruland, K.W., 1998. The complexation of 'dissolved' Cu, Zn, Cd and Pb by soluble and colloidal organic matter in Narragansett Bay. Marine Chemistry 62, 203–217.

Wen, L.-S., Stordal, M.C., Tang, D., Gill, G.A., Santschi, P.H., 2000. An ultraclean cross-flow ultrafiltration technique for the study of trace metal phase speciation in seawater. Marine Chemistry 55 (1–2), 129–152.

Wu, J.F., Luther III, G.W., 1995. Complexation of Fe(III) by natural organic ligands in the Northwest Atlantic Ocean by competitive ligand equilibration method and a kinetic approach. Marine Chemistry 50, 159–178.

Wu, J.F., Boyle, E., Sunda, W., Wen, L.S., 2001. Soluble and colloidal iron in the oligotrophic North Atlantic and North Pacific. Science 293 (5531), 847–849.